

## Theoretical study of acetylide complexes of early transition metals†

Filippo De Angelis,<sup>a</sup> Nazzareno Re,<sup>a</sup> Marzio Rosi,<sup>a</sup> Antonio Sgamellotti<sup>\*a</sup> and Carlo Floriani<sup>b</sup><sup>a</sup> Dipartimento di Chimica, Università di Perugia, via Elce di Sotto 8, I-06123 Perugia, Italy<sup>b</sup> Institut de Chimie Minérale et Analytique, BCH Université de Lausanne, CH-1015, Lausanne, Switzerland

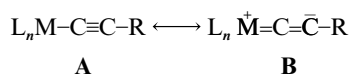
Density-functional calculations have been carried out on the series of acetylide complexes  $[M(C_2H)(OH)_3]$  with  $M = Ti, V$ , or  $Cr$  to study the electronic structure and the bonding of the  $HC\equiv C^-$  moiety to early transition-metal fragments. Analogous calculations have been performed on a typical acetylide complex of late transition metals,  $[Fe(C_2H)(\eta-C_5H_5)(CO)_2]$ , to compare bonding and reactivity of these two classes of complexes.

There is a considerable current interest in the organometallic acetylide complexes. Indeed, the acetylide anion,  $HC\equiv C^-$ , presents a large variety of interaction modes with transition metals and is susceptible to both electrophilic and nucleophilic attack allowing for further transformations and ready functionalization.<sup>1,2</sup> Moreover, acetylide complexes are becoming important in several applied fields, like organic and organometallic synthesis,<sup>3,4</sup> homo- and hetero-geneous catalysis<sup>5</sup> and material science.<sup>6</sup> The great majority of acetylide complexes are formed by middle to late transition metals, while those of early transition metals are still scarce and poorly characterized.<sup>1,7–11</sup>

Considerable knowledge has been obtained of the chemistry and reactivity of late transition-metal acetylides.<sup>1,2</sup> These complexes are highly reactive and susceptible to nucleophilic attack at the  $\alpha$ -carbon and electrophilic attack at the  $\beta$ -carbon,<sup>12</sup> see Scheme 1. This behaviour, coupled with the unsaturation of the multiple carbon–carbon bond, makes such complexes attractive as starting points for the generation of many hydrocarbyl systems including vinyl, vinylidene, alkylidene, alkylidyne and alkyl groups.

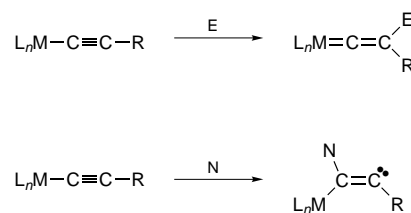
Geometric and spectroscopic features of this class of compounds suggest that the acetylide ligand is mainly a  $\sigma$  donor. The observed  $M-C$  and  $C-C$  bond lengths do not indicate substantial  $\pi$  contribution for the metal–carbon bond or bond-order reduction of the triple carbon–carbon bond, while the infrared spectra indicate slightly reduced  $\nu(C\equiv C)$  stretching frequencies. Simple considerations suggest that the  $d_\pi$  to  $\pi^*(C\equiv C)$  back donation should be favoured by late transition metals in low oxidation states but in the few cases where such  $\sigma$ -acceptor/ $\pi$ -donor synergism is observed it is only weakly established.<sup>1</sup>

The reactivity of the acetylide ligand has been intuitively rationalized on the basis of the possible resonance form **B**.

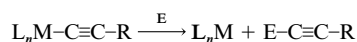


Therefore, the more electron releasing the metal centre the more enhanced is the nucleophilicity at the  $\beta$ -carbon. Theoretical calculations on manganese and iron complexes have predicted that  $\pi$  back bonding from the metal to ligand is negligible because of the high energy of the acetylide  $\pi^*$  levels.<sup>13,14</sup> Such calculations also permitted explanation of the observed regioselectivity in terms of different localization of the highest occupied (HOMO) and lowest unoccupied molecular orbital (LUMO) on the  $C_\alpha$  and  $C_\beta$  carbon atoms.

Much less is known about early transition-metal acetylides. The only structurally characterized examples of Group 4 and 5



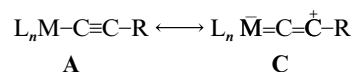
Scheme 1



Scheme 2

metals are those consisting of bent-metallocene fragments.<sup>1,7–11</sup> This is probably due to the lack of steric bulk of the acetylide ligands that may allow high reactivity at these highly electron-deficient metal centres.<sup>15,16</sup> In the few studied cases the reactivity of these complexes appears different from that observed for the electron-rich late transition-metal complexes. In particular the acetylide ligands were found to react with organic electrophiles at the  $\alpha$ -carbon,<sup>9,11</sup> and not at the  $\beta$ -carbon as observed for late transition-metal acetylides, see Scheme 2.

Such an effect has been intuitively explained by invoking the contribution of the resonance form **C** which leads to a higher



electron density on the  $C_\alpha$  carbon atom.<sup>7</sup> These complexes have  $d_\pi$  vacant orbitals available for conjugative interaction with the  $\pi$  system of the carbon–carbon triple bond; however no clear evidence for such ligand to metal  $\pi$  donation has been observed.

A very limited number of theoretical investigations has been performed on acetylide complexes,<sup>13,14,17</sup> mainly on late transition-metal complexes. In particular, in spite of the interest recently drawn by early transition-metal acetylides, no general and accurate calculations have been performed on this class of complexes to clarify the nature of the  $M-C$  bond and to study their reactivity. This paper addresses the theoretical study of the class of early transition-metal acetylides. We have performed LCAO (linear combination of atomic orbitals) density functional calculations on a series of  $[M(C_2H)(OH)_3]$  complexes with  $M = Ti$  **1**,  $V$  **2** or  $Cr$  **3** (see Fig. 1) as models of the class of acetylide complexes constituted by early transition metals in high oxidation states with  $\pi$ -donor ligands. A special emphasis is placed on the eventual metal–carbon conjugative interactions and to explain the observed reactivity pattern. The shift of  $M$  from  $Ti$  to  $Cr$  permitted us to investigate the effect of the change of the nature of the transition metal and of the vari-

† Non-SI unit employed:  $eV \approx 1.60 \times 10^{-19}$  J.

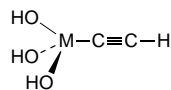


**Fig. 1** Geometrical structure of the model complexes

ation of the fragment d configuration. We have found optimized structures consistent with  $\sigma$ -bound acetylide ligands and little evidence for  $\pi$  interaction between the metal centre and the carbon–carbon multiple bond. Moreover, the observed regioselectivity towards electrophilic attack has been interpreted in terms of both charge distribution and spatial localization of the HOMO orbital. We also considered the complex  $[\text{Fe}(\text{C}_2\text{H})(\eta\text{-C}_5\text{H}_5)(\text{CO})_2]$  **4** as a typical acetylide complex of the late transition metals in order to make a comparison with the properties calculated for the early transition-metal complexes studied in this work.

## Computational Details

The calculations were performed by the GAUSSIAN 94 program package<sup>18</sup> on IBM RISC/6000 workstations. The B3LYP hybrid exchange–correlation functional was used for all the calculations. This is based on Becke's three-parameter functional<sup>19</sup> including an Hartree–Fock exchange contribution with a non-local correction for the exchange potential proposed by Becke in 1988<sup>20</sup> together with the non-local correction for the correlation energy provided by Lee *et al.*<sup>21</sup> Molecular structures were optimized using the B3LYP functional. It had been demonstrated that this hybrid functional gives accurate optimized geometries for a wide range of molecules.<sup>22</sup>

We used two basis sets for the calculations on complexes **1–3**, based on the 6-311G set<sup>23</sup> for carbon and hydrogen atoms and the Wachters–Hay set<sup>24</sup> for the transition-metal atoms. The first basis set, hereafter referred to as **I**, includes a set of d polarization functions on the two acetylide carbon atoms. The second set, **II**, includes three sets of d and one set of f polarization functions on the two carbons, one set of p functions on the hydrogen atoms, and two sets of f and one set of g polarization functions on the transition metals.

Full geometry optimizations were performed on complexes **1–3** in  $C_{3v}$  symmetry with the two basis sets. The results for the two basis sets were quite similar and only those obtained with basis set **II** will be discussed. Only the main geometrical parameters pertaining to the metal–acetylide bonding were optimized on complex **4** using the basis set **I**. Mulliken analyses were performed using basis set **I**, with polarization functions only on the acetylide carbon atoms. The coordinate system has been chosen so that the  $z$  axis is in the M–C–C direction.

## Results and Discussion

The ground states found for the complexes of Ti and V are respectively a singlet  $^1\text{A}_1$  and a doublet  $^2\text{A}_1$ . For the chromium complex we optimized the structure of both the lowest singlet and triplet state. The triplet  $^3\text{A}_1$  was found as the ground state with the singlet  $^1\text{A}_1$  169.3 kJ mol<sup>−1</sup> higher in energy.

The optimized geometrical parameters for complexes **1–3** are reported in Table 1. The metal–carbon distances, although slightly short still lie in the ranges expected for a single  $\text{M}^{\text{IV}}\text{--C}_{\text{sp}}$  bond on the basis of the covalent radii. A direct comparison with the few experimental data available for this class of compound is not possible as the ligands employed in the calculations (hydroxo) differ from those of the experimentally characterized compounds (mainly cyclopentadienyl). However, the calculated C–C bond distances are all around 1.21 Å, in agreement with the few available data and with the value for free acetylene (1.21 Å).

The computed main valence-energy levels, labelled according to  $C_{3v}$  symmetry, are reported in Table 2 together with the fragment population analysis. The calculated gross Mulliken

**Table 1** Geometrical parameters of titanium, vanadium and chromium complexes in  $C_{3v}$  symmetry. Basis set **II**. Bond lengths in Å, angles in °

Parameter	$[\text{Ti}(\text{C}_2\text{H})(\text{OH})_3]$	$[\text{V}(\text{C}_2\text{H})(\text{OH})_3]$	$[\text{Cr}(\text{C}_2\text{H})(\text{OH})_3]$	
			$^3\text{A}_1$	$^1\text{A}_1$
C–H	1.065	1.065	1.064	1.064
C–C	1.212	1.212	1.210	1.215
M–C	2.052	1.969	1.919	1.882
M–O	1.786	1.755	1.746	1.748
O–H	0.965	0.966	0.972	0.973
O–M–C	107.5	104.7	101.3	100.9
M–O–H	180.0	141.4	125.0	124.7
O–M–O	111.3	113.8	116.2	116.5

**Table 2** Energy and composition of the frontier orbitals for the complexes **1–3**

Complex	Orbital	$E/\text{eV}$	Composition (%)			
			$\text{C}_\alpha$	$\text{C}_\beta$	M	(OH) <sub>3</sub>
$[\text{Ti}(\text{C}_2\text{H})(\text{OH})_3]$	8e	−7.53	39	44	3	14
	9e	−2.09	5	13	60	22
$[\text{V}(\text{C}_2\text{H})(\text{OH})_3]$	8e	−7.61	28	34	7	31
	15a <sub>1</sub>	−5.99	2	12	61	25
	2a <sub>2</sub>	−1.40	2	9	67	22
$[\text{Cr}(\text{C}_2\text{H})(\text{OH})_3]$	8e	−7.61	17	18	15	50
	9e	−6.73	8	20	44	28
	10e	−2.88	1	1	58	40
	15a <sub>1</sub>	−1.79	28	20	39	13

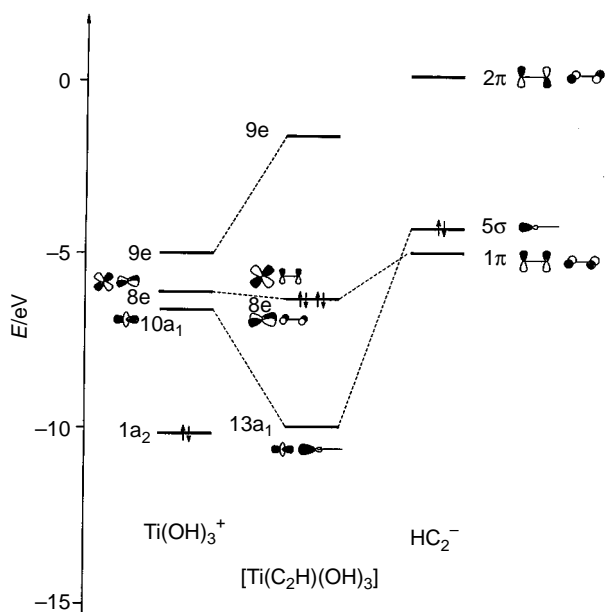
**Table 3** Mulliken charges on the acetylide carbons and the metal for complexes **1–4**

Complex	$Q(\text{C}_\alpha)$	$Q(\text{C}_\beta)$	$Q(\text{M})$
$[\text{Ti}(\text{C}_2\text{H})(\text{OH})_3]$	−0.49	−0.33	1.90
$[\text{V}(\text{C}_2\text{H})(\text{OH})_3]$	−0.44	−0.34	1.82
$[\text{Cr}(\text{C}_2\text{H})(\text{OH})_3]$ ( $^3\text{A}_1$ )	−0.43	−0.34	1.80
$[\text{Fe}(\text{C}_2\text{H})(\eta\text{-C}_5\text{H}_5)(\text{CO})_2]$	−0.33	−0.45	1.00

charges on the acetylide carbon atoms and on the metal are reported in Table 3. A qualitative bonding picture for these  $[\text{M}(\text{CCH})(\text{OH})_3]$  complexes can be discussed by a fragment approach in which the  $\text{HCC}^-$  unit and the  $(\text{HO})_3\text{M}^+$  metal fragment interact along the MCC axis ( $z$  axis in our coordinate system). The acetylide  $\text{HC}\equiv\text{C}^-$  fragment has been considered in its  $^1\Sigma^+$  ground state, with configuration  $(4\sigma)^2(1\pi)^4(5\sigma)^2$ , and its main valence orbitals are a degenerate set of  $\pi$  orbitals describing the C–C  $\pi$  bond ( $1\pi$ ), a degenerate set of  $\pi$  antibonding orbitals ( $2\pi$ ) and a  $\sigma$  orbital describing the lone pair of the carbon atom ( $5\sigma$ ). The electronic structure of the  $(\text{HO})_3\text{M}^+$  metal fragments easily can be understood if we consider them as pseudo-tetrahedral complexes with one ligand removed. Their valence orbitals consist of a low-lying group of three doubly occupied MOs describing the M–O bonds and a high-lying group of five orbitals of mainly metal d character, unoccupied or singly occupied depending on the d configuration of the metal. In more detail, the d orbitals are made up of  $10a_1$ , which is essentially an  $s\text{--}d_{z^2}$  hybrid, a doubly degenerate  $8e$ , the components of which are mainly metal  $d_{xz}$  and  $d_{yz}$  orbitals of  $d_\pi$  character, and a double degenerate  $9e$ , with components of mainly  $d_{x^2-y^2}$  and  $d_{xy}$  orbitals of  $d_\delta$  character. However in the  $C_{3v}$  symmetry, the  $d_\pi$  and the  $d_\delta$  components can mix and, actually, the  $8e$  and  $9e$  orbitals have small  $d_\delta$  and  $d_\pi$  components, respectively. This picture is in agreement with the usual qualitative description of the  $C_{3v}$   $\text{ML}_3$  fragment based on extended Hückel calculations.<sup>25</sup> Fig. 2 shows the MOs for the metallic fragment interaction with the MOs of the  $\text{HC}\equiv\text{C}^-$  unit to reproduce the higher levels of the  $[\text{Ti}(\text{C}_2\text{H})(\text{OH})_3]$  complex **1**,

**Table 4** The  $\sigma$  and  $\pi$  populations on the acetylide carbons

Compound	$\sigma(C_\alpha)$	$\sigma(C_\beta)$	$\sigma$ Total	$\pi(C_\alpha)$	$\pi(C_\beta)$	$\pi$ Total
HCCH	4.223	4.223	8.446	1.985	1.985	3.97
[Ti(C <sub>2</sub> H)(OH) <sub>3</sub> ]	4.554	4.319	8.873	1.91	1.98	3.89
[V(C <sub>2</sub> H)(OH) <sub>3</sub> ]	4.497	4.317	8.814	1.91	2.00	3.91
[Cr(C <sub>2</sub> H)(OH) <sub>3</sub> ] ( <sup>3</sup> A <sub>1</sub> )	4.466	4.327	8.793	1.94	1.98	3.92
[Fe(C <sub>2</sub> H)( $\eta$ -C <sub>5</sub> H <sub>5</sub> )(CO) <sub>2</sub> ]	4.357	4.337	8.694	1.92	2.09	4.01

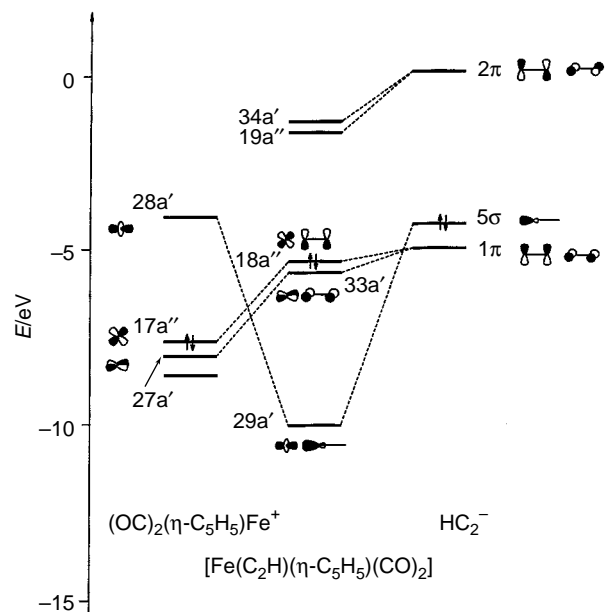
**Fig. 2** Molecular orbital diagram for the [Ti(C<sub>2</sub>H)(OH)<sub>3</sub>] complex depicting the interactions between the frontier orbitals of (HO)<sub>3</sub>Ti<sup>+</sup> and HC<sub>2</sub><sup>-</sup> fragments

and is representative of the behaviour of all the complexes considered. Two main orbital-overlap interactions can be distinguished in Fig. 2 and Table 2: (i) a strong donation from the  $\sigma$  orbitals of acetylide to the empty metal  $d_{z^2}$  which forms the metal–carbon  $\sigma$  bond; (ii) a small donation from the  $\pi$  orbitals of acetylide into empty  $d_{xz}$  and  $d_{yz}$  orbitals of the metal. This latter interaction gives a small  $\pi$  contribution to the metal–carbon bond and leads to a HOMO orbital which is mainly composed of acetylide  $\pi$  orbitals with a small  $d_{\pi}$  contribution.

The bonding picture above can be extended to complexes 2 and 3 with minor differences due to the extra unpaired electrons. The highest doubly occupied orbitals are again mainly acetylide  $\pi$  orbitals while the singly occupied orbitals are predominantly of metal  $3d_{\pi}$  character. For all the complexes the LUMOs are almost entirely localized on the metal fragments.

Better to understand the acetylide to metal donation, we performed a population analysis of the molecular orbitals by calculating the  $\sigma$  and  $\pi$  population on the C $\equiv$ C acetylide fragment, and the results are shown in Table 4. The  $\sigma$  populations on the two carbon atoms are slightly different due to the larger localization of the  $\sigma$  orbital on the  $\alpha$ -carbon. The computed values show a reduction of the  $\sigma$  populations moving from Ti to Fe due to the lowering in energy of the  $d_{z^2}$  orbital of the metal, which is mostly responsible for the  $\sigma$  interaction between the metal and the acetylide fragment.

A  $\pi$  donation from the  $\pi$  orbitals of the HC $\equiv$ C<sup>-</sup> moiety towards the empty  $d_{\pi}$  orbitals of the metal would reduce the value of the  $\pi$  population of the HC $\equiv$ C moiety from that found for the acetylene molecule (3.97). The results of the population analysis show a small reduction of the computed  $\pi$  populations, 0.08, 0.06 and 0.05 for Ti, V and Cr, respectively, and suggest a very small  $\pi$  donation. Such a small  $\pi$  donation is presumably due to the large energy difference between the acetylide  $\pi$  orbitals and the empty  $d_{\pi}$  of the metal fragments. This result is

**Fig. 3** Molecular orbital diagram for the [Fe(C<sub>2</sub>H)( $\eta$ -C<sub>5</sub>H<sub>5</sub>)(CO)<sub>2</sub>] complex depicting the interactions between the frontier orbitals of (OC)<sub>2</sub>( $\eta$ -C<sub>5</sub>H<sub>5</sub>)Fe<sup>+</sup> and HC<sub>2</sub><sup>-</sup> fragments

consistent with the computed lengths for both the metal–carbon bonds, which lie in the range of single bonds or are at most very slightly shorter, and the carbon–carbon bond lengths which are all around 1.21 Å. On the other hand, a high  $\pi$  donation would lead to a more remarkable reduction of the metal–carbon bond distance from the value of a typical single bond and lengthening of the C–C bond length.

Density functional calculations have been performed on the [Fe(C<sub>2</sub>H)( $\eta$ -C<sub>5</sub>H<sub>5</sub>)(CO)<sub>2</sub>] molecule 4. Only the main geometrical parameters pertaining to the metal–acetylide bonding were optimized and Fe–C and C–C distances in agreement with the experimental values for [Fe(C<sub>2</sub>Ph)( $\eta$ -C<sub>5</sub>H<sub>5</sub>)(CO)<sub>2</sub>]<sup>26</sup> were obtained (1.901 and 1.220 vs. 1.920 and 1.201 Å, respectively). The computed valence-energy levels, labelled according to  $C_s$  symmetry, are reported in Table 5. Fig. 3 shows the interaction between the (OC)<sub>2</sub>( $\eta$ -C<sub>5</sub>H<sub>5</sub>)Fe<sup>+</sup> fragment and the acetylide H–C $\equiv$ C<sup>-</sup> fragment. Two main orbital interactions are observed as for complexes 1–3. However, although a similar  $\sigma$  donation from the acetylide  $\sigma$  orbital to an empty  $d_{z^2}$  orbital is found, a different situation is observed for the  $\pi$  interaction as a consequence of the low-energy  $d_{\pi}$  orbitals of the iron fragment (27a' and 17a''). These two filled orbitals have the right symmetry to interact with both the  $\pi$  and  $\pi^*$  acetylide orbitals but, as the  $\pi^*$  are far higher in energy, they give essentially a destabilizing two-orbital four-electron interaction with the filled  $\pi$  orbitals. Moreover, the HOMO has now a major  $d_{\pi}$  character with a minor contribution from the  $\pi$  orbital of acetylide. The analysis of the  $\pi$  population on the HC $\equiv$ C moiety reported in Table 4 shows a small increase with respect to the acetylene molecule (+0.04) indicating a negligible metal to acetylide  $\pi$  donation and therefore an essentially single metal–carbon bond in agreement with the experimental evidence.<sup>26</sup>

Besides the electronic structure of these compounds, we have studied their reactivity and regioselectivity towards nucleophilic

**Table 5** Energy and composition of the frontier orbitals for the complex  $[\text{Fe}(\text{C}_2\text{H})(\eta\text{-C}_5\text{H}_5)(\text{CO})_2]$

Orbital	<i>E</i> /eV	Composition (%)			
		$\text{C}_\alpha$	$\text{C}_\beta$	Fe	$(\eta\text{-C}_5\text{H}_5)(\text{CO})_2$
18a''	−6.03	11	34	34	21
19a''	−2.23	6	2	30	62

and electrophilic additions. We followed the approach of Fukui *et al.*,<sup>27</sup> further generalized by Klopman<sup>28</sup> which distinguishes between charge-controlled chemical reactions, where the regioselectivity is determined by the charge distribution, and frontier-controlled reactions, where regioselectivity is determined by the frontier-orbital localization.

The reactivity and regioselectivity for the late transition-metal acetylides towards electrophiles (directed towards the  $\beta$ -carbon) was interpreted in terms of charge and orbital factors in concert, while the regioselectivity towards nucleophilic attack (directed to the  $\alpha$ -carbon) was attributed to the localization of the LUMO orbital on the  $\alpha$ -carbon.<sup>13</sup> Our accurate density-functional calculations on the  $[\text{Fe}(\text{C}_2\text{H})(\eta\text{-C}_5\text{H}_5)(\text{CO})_2]$  molecule confirm the results of Kostić and Fenske<sup>13</sup> obtained through much less accurate Fenske–Hall calculations. For complex **4** the HOMO and LUMO orbitals are the 18a'' and 19a'' orbitals, respectively. Indeed, Tables 3 and 5 show that: (i) the negative charge is much higher on the  $\beta$ -carbon and also the HOMO orbital is mainly localized on it; (ii) the LUMO orbital is mainly localized on the  $\alpha$ -carbon causing the regioselectivity of the nucleophilic attack.

Only few experimental data are available on the reactivity of early transition-metal acetylides toward electrophilic attack, and indicate that these complexes react with organic electrophiles at the  $\alpha$ -carbon.<sup>9,11</sup> There is no evidence for electrophilic attack at the  $\beta$ -carbon observed in late transition-metal acetylides. To explain the different regioselectivity toward electrophilic attack shown by early transition-metal acetylides, we have analysed both atomic charges and localization of the HOMO in complexes **1–3**. The localization of the frontier orbitals is indicated by the composition of the molecular orbitals in Table 2. For **1–3** the HOMO orbitals are the 8e orbitals while the LUMO orbitals are the 9e, 2a<sub>2</sub> and 15a<sub>1</sub> respectively.

Table 3 shows that the  $\alpha$ -carbon bears a higher negative charge than the  $\beta$ -carbon for all three complexes considered. From Table 2 we can instead notice how the HOMO is slightly more localized on the  $\beta$ -carbon, although the difference is quite small. However, these HOMO orbitals are not well separated, but close (about 1 eV) to a few doubly occupied MOs slightly more localized on the  $\alpha$ -carbon. Thus the above results suggest that the observed electrophilic attack at the  $\alpha$ -carbon is determined by charge factors. This interpretation is confirmed by the low energy of the HOMO for **1–3** (ca. −7.5 eV), lower than that for the late transition-metal acetylide **4** (ca. −6.0 eV). Indeed, the energy difference between these HOMOs and the LUMOs of typical electrophilic species is high enough to give a negligible charge-transfer contribution to the perturbation expression of the interaction energy<sup>28</sup> and therefore make the interaction charge controlled.

The regioselectivity of complexes **1–3** towards nucleophilic attack can be easily interpreted with the same approach. Indeed, Table 3 shows a high positive charge on the metal atoms, while Table 2 shows that the lowest unoccupied molecular orbitals are essentially localized on the metals. Therefore both orbital and charge factors indicate high reactivity of this metal centre towards nucleophilic attack. This result is consistent with the scarcity of early transition-metal (especially Groups 4 and 5) acetylides, the structurally characterized examples of which are limited to bent-metallocene fragments in

which the nucleophilic attack on the metal is prevented by the bulky pentadienyl ligands.<sup>1</sup>

## Conclusion

The main purpose of the present investigation has been to clarify the nature of the metal–carbon bond in early transition-metal acetylides and to explain their observed reactivity pattern. Our density-functional calculations on the series of  $[\text{M}(\text{C}_2\text{H})(\text{OH})_3]$  complexes have shown little evidence of  $\pi$  interaction between the metal centre and the carbon–carbon multiple bond. The observed regioselectivity for electrophilic attack (on the  $\alpha$ -carbon) has been recognized as charge controlled.

## Acknowledgements

This work has been carried out within the COST D3 Action. One of us (N. R.) thanks the Fondation Herbette (Lausanne) for a fellowship.

## References

- 1 R. Nast, *Coord. Chem. Rev.*, 1982, **47**, 89.
- 2 M. I. Bruce and A. G. Swincer, *Adv. Organomet. Chem.*, 1983, **22**, 59; M. I. Bruce, *Chem. Rev.*, 1991, **91**, 197.
- 3 M. I. Bruce, *Pure Appl. Chem.*, 1986, **58**, 553.
- 4 K. M. Nicholas, M. O. Nestle and D. Seyferth, in *Transition Metal Organometallics in Organic Synthesis*, ed. H. Alper, Academic Press, New York, 1978, vol. 2, ch. 1.
- 5 D. H. Barry and R. Eisenberg, *Organometallics*, 1987, **6**, 1796 and refs. therein.
- 6 K. Sonogashira, K. Ohga, S. Takahashi and N. Hagihara, *J. Organomet. Chem.*, 1980, **188**, 237.
- 7 G. Erker, W. Fröberg, R. Benn, R. Mynott, K. Angermund and C. Krüger, *Organometallics*, 1989, **8**, 991.
- 8 H. Lang and D. Z. Seyferth, *Z. Naturforsch. Teil B*, 1990, **212**, 45.
- 9 J. H. Teuben and H. J. DeLiefde Meijer, *J. Organomet. Chem.*, 1968, **15**, 131.
- 10 W. J. Evans, I. Bloom and R. J. Doedens, *J. Organomet. Chem.*, 1984, **265**, 249.
- 11 H. Kawaguchi and K. Tatsumi, *Organometallics*, 1995, **14**, 4294.
- 12 A. Davison and J. P. Selegue, *J. Am. Chem. Soc.*, 1980, **102**, 2455.
- 13 N. M. Kostić and R. F. Fenske, *Organometallics*, 1982, **1**, 974.
- 14 D. L. Lichtenberger, S. K. Renshaw and R. M. Bullock, *J. Am. Chem. Soc.*, 1993, **115**, 3276.
- 15 W. J. Evans, R. A. Keyer and J. W. Ziller, *Organometallics*, 1993, **12**, 2618.
- 16 H. Heeres and J. H. Teuben, *Organometallics*, 1991, **10**, 1980.
- 17 E. T. Knight, L. K. Myers and M. E. Thompson, *Organometallics*, 1992, **11**, 3691.
- 18 GAUSSIAN 94, Revision A.1, M. J. Frisch, G. W. Trucks, H. M. Schlegel, P. M. W. Gill, B. G. Johnson, M. W. Wong, J. B. Foresman, M. A. Robb, M. Head-Gordon, E. S. Replogle, R. Gomperts, J. L. Andres, K. Raghavachari, J. S. Binkley, C. Gonzales, R. L. Martin, D. J. Fox, D. J. Defrees, J. Baker, J. J. P. Stewart and J. A. Pople, GAUSSIAN Inc., Pittsburgh, PA, 1994.
- 19 A. D. Becke, *J. Chem. Phys.*, 1993, **98**, 5648.
- 20 A. D. Becke, *Phys. Rev. A*, 1988, **38**, 2398.
- 21 C. Lee, W. Young and R. G. Parr, *Phys. Rev. B*, 1988, **37**, 785.
- 22 C. W. Bauschlicher jun., *Chem. Phys. Lett.*, 1995, **246**, 40.
- 23 M. J. Frisch, J. A. Pople and J. S. Binkley, *J. Chem. Phys.*, 1984, **80**, 3265 and refs. therein.
- 24 A. J. H. Wachters, *J. Chem. Phys.*, 1970, **52**, 1033; P. J. Hay, *J. Chem. Phys.*, 1977, **77**, 4377.
- 25 T. A. Albright, J. K. Burdett and M.-H. Whangbo, *Orbital Interaction in Chemistry*, Wiley, New York, 1986.
- 26 R. Goddard, J. Howard and P. Woodward, *J. Chem. Soc., Dalton Trans.*, 1974, 2025.
- 27 K. Fukui, T. Yonezawa and C. Nagata, *J. Chem. Phys.*, 1957, **27**, 1247; 1959, **31**, 550; K. Fukui, *Theory of Orientation and Stereoselection*, Springer, Berlin, 1975.
- 28 G. Klopman and R. F. Hudson, *Theor. Chim. Acta*, 1967, **8**, 1965; G. Klopman, *J. Am. Chem. Soc.*, 1968, **90**, 223; G. Klopman, in *Chemical Reactivity and Reaction Paths*, ed. G. Klopman, Wiley, New York, 1974, pp. 59–67.

Received 7th April 1997; Paper 7/02369C